Aberystwyth University

Genome-wide association studies and prediction of 17 traits related to phenology, biomass and cell wall composition in the energy grass Miscanthus sinensis

Slavov, Gancho T; Nipper, Rick; Robson, Paul; Farrar, Kerrie; Allison, Gordon G; Bosch, Maurice; Clifton-Brown, John C; Donnison, Iain S; Jensen, Elaine

Published in:
New Phytologist

DOI:
10.1111/nph.12621

Publication date:
2014

Citation for published version (APA):
Slavov, G. T., Nipper, R., Robson, P., Farrar, K., Allison, G. G., Bosch, M., Clifton-Brown, J. C., Donnison, I. S., & Jensen, E. (2014). Genome-wide association studies and prediction of 17 traits related to phenology, biomass and cell wall composition in the energy grass Miscanthus sinensis. *New Phytologist*, *201*(4), 1227-1239. https://doi.org/10.1111/nph.12621

General rights
Copyright and moral rights for the publications made accessible in the Aberystwyth Research Portal (the Institutional Repository) are retained by the authors and/or other copyright owners and it is a condition of accessing publications that users recognise and abide by the legal requirements associated with these rights.

• Users may download and print one copy of any publication from the Aberystwyth Research Portal for the purpose of private study or research.
• You may not further distribute the material or use it for any profit-making activity or commercial gain
• You may freely distribute the URL identifying the publication in the Aberystwyth Research Portal

Take down policy
If you believe that this document breaches copyright please contact us providing details, and we will remove access to the work immediately and investigate your claim.

tel: +44 1970 62 2400
email: is@aber.ac.uk

Download date: 09. Jul. 2020

Genome-wide association studies and prediction of 17 traits related to phenology, biomass and cell wall composition in the energy grass *Miscanthus sinensis*

Gancho T. Slavov[1], Rick Nipper[2], Paul Robson[1], Kerrie Farrar[1], Gordon G. Allison[1], Maurice Bosch[1], John C. Clifton-Brown[1], Iain S. Donnison[1] and Elaine Jensen[1]

[1]Institute of Biological, Environmental and Rural Sciences, Aberystwyth University, Aberystwyth SY23 3EB, UK; [2]Floragenex Inc., Eugene, OR 97403, USA

Author for correspondence:
Gancho T. Slavov
Tel: +44 01970 823094
Email: gts@aber.ac.uk

Received: *16 August 2013*
Accepted: *28 October 2013*

New Phytologist (2014) **201:** 1227–1239
doi: 10.1111/nph.12621

Key words: genomic selection, genome-wide association studies (GWAS), *Miscanthus sinensis*, molecular markers, RAD-Seq, single-nucleotide variants.

Summary

- Increasing demands for food and energy require a step change in the effectiveness, speed and flexibility of crop breeding. Therefore, the aim of this study was to assess the potential of genome-wide association studies (GWASs) and genomic selection (i.e. phenotype prediction from a genome-wide set of markers) to guide fundamental plant science and to accelerate breeding in the energy grass *Miscanthus*.
- We generated over 100 000 single-nucleotide variants (SNVs) by sequencing restriction site-associated DNA (RAD) tags in 138 *Micanthus sinensis* genotypes, and related SNVs to phenotypic data for 17 traits measured in a field trial.
- Confounding by population structure and relatedness was severe in naïve GWAS analyses, but mixed-linear models robustly controlled for these effects and allowed us to detect multiple associations that reached genome-wide significance. Genome-wide prediction accuracies tended to be moderate to high (average of 0.57), but varied dramatically across traits. As expected, predictive abilities increased linearly with the size of the mapping population, but reached a plateau when the number of markers used for prediction exceeded 10 000–20 000, and tended to decline, but remain significant, when cross-validations were performed across subpopulations.
- Our results suggest that the immediate implementation of genomic selection in *Miscanthus* breeding programs may be feasible.

Introduction

Cost-efficient genotyping protocols based on next-generation sequencing (Davey *et al.*, 2011) have narrowed the gap between model and non-model plants, thereby creating great opportunities in crop breeding (Hamblin *et al.*, 2011; Morrell *et al.*, 2012). Two approaches that are likely to have particularly strong and widespread impacts are the dissection of complex traits through genome-wide association studies (GWASs; Cardon & Bell, 2001) and genome-wide phenotype prediction (genomic selection; Meuwissen *et al.*, 2001). By informing fundamental science and applied breeding, respectively, these two approaches have the potential to bridge the molecular and statistical void between phenotype and genotype, thereby shedding light on key biological questions.

With increasing demands for food and energy, decreasing land base and changing environmental conditions (Foley *et al.*, 2011; Valentine *et al.*, 2012), the urgency to develop accelerated crop breeding strategies cannot be overstated. The use of lignocellulosic energy crops is one of many potential mitigating factors for this problem, but the widespread adoption of these crops has been slow and hampered by a number of technological and economic challenges, with major breakthroughs required both in terms of biomass yield on low-value lands and conversion efficiency (Sims *et al.*, 2010; Feltus & Vandenbrink, 2012; Service, 2013). Genomic approaches (e.g. GWAS and genomic selection) can substantially facilitate these breakthroughs and are therefore among the focal points in this area of research (Rubin, 2008; Feltus & Vandenbrink, 2012; Slavov *et al.*, 2013a).

The tropical C_4 grass *Miscanthus* is a promising energy crop because of its broad adaptability, potentially very high yields and low requirements for agricultural inputs (Clifton-Brown *et al.*, 2004, 2007; Hastings *et al.*, 2009). However, *Miscanthus* species are undomesticated, and several breeding programs in East Asia, Europe and North America are targeting the accelerated development of hybrids and varieties that are high yielding, can be established and maintained at low cost and have cell wall characteristics that allow efficient conversion to fuels and products. In a recent study, we used a combination of phenotypic data from a replicated field trial and 120 molecular markers to delineate an experimental population of *M. sinensis* for GWAS and genome-wide prediction (Slavov *et al.*, 2013b). This population had

© 2013 The Authors
New Phytologist © 2013 New Phytologist Trust
This is an open access article under the terms of the Creative Commons Attribution License, which permits use, distribution and reproduction in any medium, provided the original work is properly cited.

relatively weak substructure ($F_{ST} < 0.06$), but captured high levels of genetic variation across a range of phenotypic traits related to phenology, biomass productivity and cell wall composition.

Building on this study, we: (1) sequenced restriction site-associated DNA (RAD) tags in 142 *M. sinensis* genotypes and generated over 100 000 'RAD-Seq' single-nucleotide variants (SNVs); (2) confirmed patterns of putatively neutral population structure detected in our previous study, but also used the power of the RAD-Seq markers to add substantial new details, including the hypothetical geographical origins for a large number of accessions with unknown sampling locations; and (3) assessed the potential of GWASs and genome-wide prediction to guide biological discovery and accelerated breeding in *Miscanthus*.

Materials and Methods

Plant materials, phenotyping and DNA extraction

We defined an experimental population of 145 *M. sinensis* Anders. genotypes based on previous analyses of single-nucleotide polymorphism (SNP) data (Slavov *et al.*, 2013b). Of these, we attempted RAD sequencing for 142 and obtained robust data for 138 genotypes (see section on Sample clustering, population structure and relatedness), which were used for all subsequent analyses (Fig. 1). In 2005, our study population was planted at 1.5 × 1.5 m spacing in a replicated field trial located near Aberystwyth (Wales, UK), following a randomized complete block design, with one replicate per genotype in each of four blocks. The field trial has been described in greater detail in several previous studies (Allison *et al.*, 2011; Jensen *et al.*, 2011; Robson *et al.*, 2012). Phenotyping and DNA extraction protocols have been described by Slavov *et al.* (2013b). Briefly, 17 phenotypic traits reflecting (1) phenology, (2) morphology and biomass productivity, and (3) cell wall composition, were measured on plants in all four replicates of the trial 2–4 yr after establishment (Table 1, Fig. 2).

Phenotypic data analysis

Phenotypic data analyses have been described by Slavov *et al.* (2013b). Briefly, mixed linear models were used to estimate variance components and best linear unbiased predictors (BLUPs) for each trait. We also calculated phenotypic (Pearson's *r*) and genetic correlations among all pairs of traits (Fig. 2). Genetic correlations were calculated using two different approaches. For pairs of traits measured in the same year, we calculated genetic correlations from estimates of genetic covariance (i.e. using Eqn 9, as described by Howe *et al.*, 2000). Alternatively, for pairs of traits measured in different years, we calculated genetic correlations from phenotypic correlations and estimates of broad sense heritability for each trait (i.e. Eqn 8, as described by Howe *et al.*, 2000).

RAD sequencing

RAD library preparation was performed by Floragenex, Inc. (Eugene, OR, USA). Briefly, genomic DNA from each genotype was digested with the restriction endonuclease *Pst*I and processed into multiplexed RAD libraries following the methods described in previous studies (Baird *et al.*, 2008; Stölting *et al.*, 2013). *Pst*I adapters, each containing a unique 6-bp multiplex sequence index (barcode), were affixed to digested templates, polished and amplified via a polymerase chain reaction. The resulting RAD libraries were run on two Illumina (San Diego, CA, USA) HiSeq platforms at Ambry Genetics (Aliso Viejo, CA, USA) and the Oregon State University Center for Genome Research and Biocomputing (Corvallis, OR, USA) using Illumina 1 × 100-bp chemistry.

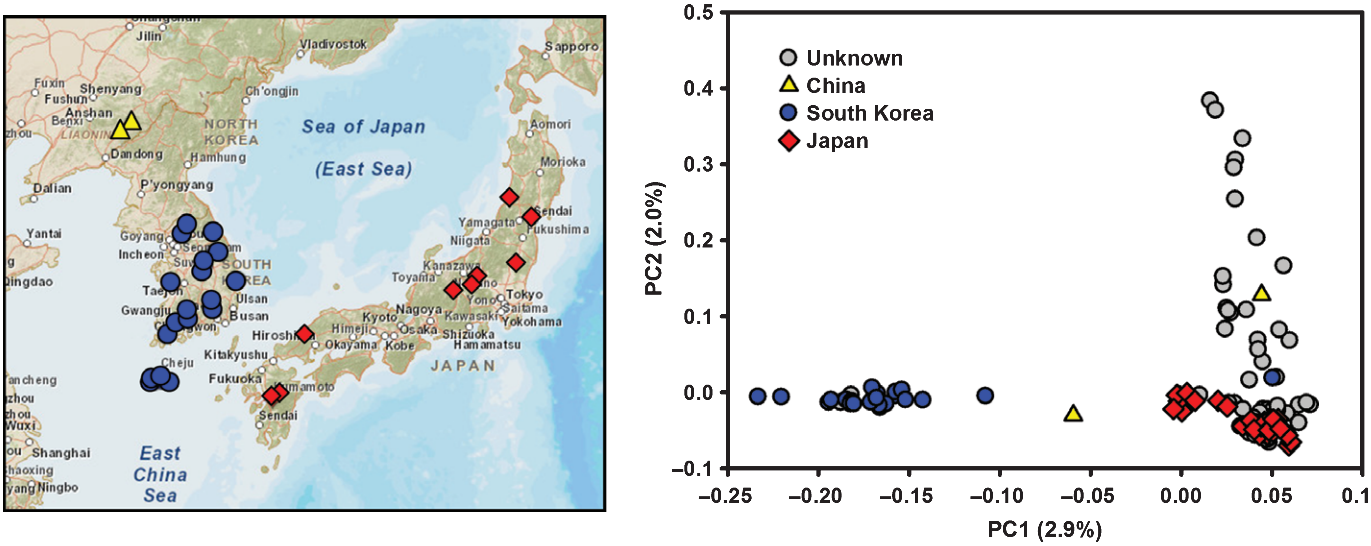

Fig. 1 Geographical distribution and principal component (PC) analysis of population genetic structure for 138 *Miscanthus sinensis* genotypes using 14 073 single-nucleotide variant loci. The percentages of the total variation explained by each PC are shown in parentheses.

© 2013 The Authors
New Phytologist © 2013 New Phytologist Trust

Table 1 Phenotypic traits measured in 142 *Miscanthus sinensis* genotypes

Trait[a]	Definition	Q_{ST}[b]	*Geo(r)*[c]	PC1 (*P* value)[d]	PC2 (*P* value)[e]
Phenology					
DOYFS1.9	Date of flowering stage 1: day of year when the first flag leaf emerged	**0.24**	**Alt (−0.66)**	**0.42 (< 0.001)**	**0.19 (0.039)**
AvgeSen.9	Average senescence score (0–10) throughout the growing season	0.04	**Lat (0.46)**	**−0.19 (0.024)**	0.03 (0.752)
Morphology/biomass					
BaseDiameter.9	Largest plant diameter measured at ground level (mm)	0.03	Long (0.18)	−0.09 (0.285)	**−0.30 (< 0.001)**
DryMatter.9	Estimated total dry weight (g)	0.01	Alt (−0.20)	−0.09 (0.295)	−0.06 (0.497)
LeafLength.7	Ligule-to-tip length along the central vein of the youngest leaf with a ligule (cm)	**0.34**	**Alt (−0.59)**	**0.46 (< 0.001)**	**0.21 (0.013)**
LeafWidth.7	Blade width at half-leaf length for the leaf used to measure *LeafLength* (cm)	0.00	Lat (−0.21)	0.09 (0.270)	**−0.27 (0.001)**
MaxCanopyHeight.9	Height from the ground to the point of 'inflection' of the majority of leaves (cm)	0.18	Lat (−0.23)	**−0.29 (0.001)**	−0.03 (0.729)
Moisture.9	Estimated moisture content based on a subsample (%)	**0.34**	**Alt (−0.66)**	**0.49 (< 0.001)**	0.01 (0.946)
StatureCategory.7	Additive combination of *StatureLeafAngle* and *StatureStemAngle*	0.02	**Long (0.37)**	**−0.19 (0.030)**	−0.16 (0.054)
StatureLeafAngle.7	Three-category score reflecting leaf angle relative to the vertical	0.06	Alt (0.19)	−0.16 (0.059)	**0.18 (0.035)**
StatureStemAngle.7	Four-category score reflecting stem angle relative to the vertical	0.00	**Long (0.36)**	−0.15 (0.081)	**−0.20 (0.017)**
StemDiameter.9	Diameter 10–15 cm from the ground of a randomly chosen stem (mm)	0.00	**Alt (−0.25)**	0.08 (0.375)	−0.08 (0.332)
TallestStem.9	Length of the tallest stem (cm)	**0.46**	**Alt (0.57)**	**−0.53 (< 0.001)**	−0.08 (0.361)
TransectCount.9	Number of stems with ≥ 50% canopy height across the middle of the plant	0.00	Lat (0.19)	0.08 (0.370)	0.02 (0.787)
Cell wall composition					
Cellulose.8	Gravimetrically measured cellulose content (% dry weight)	**0.23**	**Alt (0.54)**	**−0.41 (< 0.001)**	0.02 (0.793)
Hemicellulose.8	Gravimetrically measured hemicellulose content (% dry weight)	0.06	Long (0.22)	**−0.21 (0.015)**	0.13 (0.117)
Lignin.8	Gravimetrically measured lignin content (% dry weight)	0.00	Long (−0.17)	0.00 (0.959)	0.03 (0.770)

[a] Trait, phenotypic traits measured in 2007 (.7), 2008 (.8) or 2009 (.9) (i.e. after two, three or four growing seasons, respectively). Detailed phenotyping protocols have been described by Slavov et al. (2013b).

[b] Q_{ST}, genetic differentiation between 'Continent' and 'Japan' subpopulations. Values exceeding the empirical 95th percentile of putatively neutral differentiation (i.e. $F_{ST} = 0.23$) are shown in bold (Slavov et al., 2013b).

[c] *Geo(r)*, geographical coordinate with strongest correlation and Pearson's correlation coefficient (Slavov et al., 2013b). Values with two-sided $P < 0.05$ are shown in bold.

[d] PC1 (*P* value), Pearson's correlation with the first eigenvector of population structure (Fig. 1) and two-sided *P* value. Values with two-sided $P < 0.05$ are shown in bold.

[e] PC2 (*P* value), Pearson's correlation with the second eigenvector of population structure (Fig. 1) and two-sided *P* value. Values with two-sided $P < 0.05$ are shown in bold.

RAD-Seq data analysis

Sequencing adaptors and barcodes were removed using Floragenex software tools, resulting in 94-bp RAD fragments. These trimmed fragments were then aligned to a reference genome sequence using Bowtie (Langmead *et al.*, 2009), and variants were called using SAMtools (Li *et al.*, 2009). The alignment and variant calling steps were repeated twice, using different reference sequences. First, we aligned all 94-bp RAD sequences from each genotype to v 1.0 of the *Sorghum bicolor* genome (Paterson *et al.*, 2009) and parsed the resulting SAMtools pileup files using custom scripts. In a second analysis, we created a skeleton *Miscanthus* pseudo-reference of RAD sequence data (Supporting Information Methods S1). This assembly contained 48 426 clustered RAD sequences, representing *c.* 4.1 Mb of *Miscanthus* genomic sequence. To further reduce the potential of identifying spurious SNVs from low-quality sequences, reads were trimmed from the 3′ end to a total length of 85 bp. SNV detection then proceeded as described previously. These two approaches resulted in the initial identification of 142 539 and 223 046 SNVs, respectively.

We used custom scripts and VCFtools (Danecek *et al.*, 2011) to further filter SNV data based on alignment statistics, minor allele frequency (MAF) and conformity of genotype frequencies to Hardy–Weinberg expectations (Table 2). For initial data analyses aimed at validating data quality and detecting patterns of population genetic structure, we generated sets of SNVs that passed relatively stringent filtering criteria, but without restricting MAFs (i.e. 'stringent' filtering, Table 2). To enhance the power of GWAS analyses and to assess the accuracy of genome-wide prediction as a function of the number of markers used, we also generated larger sets of SNVs using 'liberal' filtering criteria (Table 2). We used the PLINK software tool (Purcell *et al.*, 2007) to calculate the number of unlinked SNVs (*plink … –indep-pairwise 50 5 0.2*), as well as to estimate linkage disequilibrium (LD) (*plink … –ld-window-r2*).

Sample clustering, population structure and relatedness

We used the individual-based principal component analysis (PCA) approach of Patterson *et al.* (2006) to detect outliers and to characterize population genetic structure based on SNV data

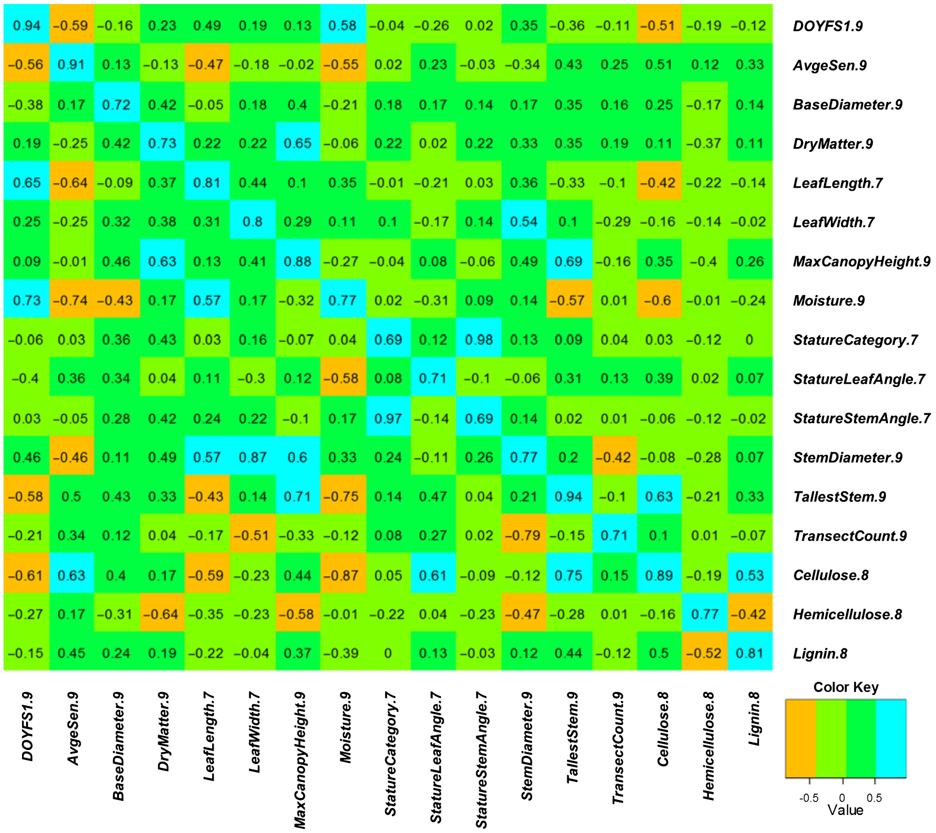

	DOYFS1.9	AvgeSen.9	BaseDiameter.9	DryMatter.9	LeafLength.7	LeafWidth.7	MaxCanopyHeight.9	Moisture.9	StatureCategory.7	StatureLeafAngle.7	StatureStemAngle.7	StemDiameter.9	TallestStem.9	TransectCount.9	Cellulose.8	Hemicellulose.8	Lignin.8
DOYFS1.9	0.94	−0.59	−0.16	0.23	0.49	0.19	0.13	0.58	−0.04	−0.26	0.02	0.35	−0.36	−0.11	−0.51	−0.19	−0.12
AvgeSen.9	−0.56	0.91	0.13	−0.13	−0.47	−0.18	−0.02	−0.55	0.02	0.23	−0.03	−0.34	0.43	0.25	0.51	0.12	0.33
BaseDiameter.9	−0.38	0.17	0.72	0.42	−0.05	0.18	0.4	−0.21	0.18	0.17	0.14	0.17	0.35	0.16	0.25	−0.17	0.14
DryMatter.9	0.19	−0.25	0.42	0.73	0.22	0.22	0.65	−0.06	0.22	0.02	0.22	0.33	0.35	0.19	0.11	−0.37	0.11
LeafLength.7	0.65	−0.64	−0.09	0.37	0.81	0.44	0.1	0.35	−0.01	−0.21	0.03	0.36	−0.33	−0.1	−0.42	−0.22	−0.14
LeafWidth.7	0.25	−0.25	0.32	0.38	0.31	0.8	0.29	0.11	0.1	−0.17	0.14	0.54	0.1	−0.29	−0.16	−0.14	−0.02
MaxCanopyHeight.9	0.09	−0.01	0.46	0.63	0.13	0.41	0.88	−0.27	−0.04	0.08	−0.06	0.49	0.69	−0.16	0.35	−0.4	0.26
Moisture.9	0.73	−0.74	−0.43	0.17	0.57	0.17	−0.32	0.77	0.02	−0.31	0.09	0.14	−0.57	0.01	−0.6	−0.01	−0.24
StatureCategory.7	−0.06	0.03	0.36	0.43	0.03	0.16	−0.07	0.04	0.69	0.12	0.98	0.13	0.09	0.04	0.03	−0.12	0
StatureLeafAngle.7	−0.4	0.36	0.34	0.04	0.11	−0.3	0.12	−0.58	0.08	0.71	−0.1	−0.06	0.31	0.13	0.39	0.02	0.07
StatureStemAngle.7	0.03	−0.05	0.28	0.42	0.24	0.22	−0.1	0.17	0.97	−0.14	0.69	0.14	0.02	0.01	−0.06	−0.12	−0.02
StemDiameter.9	0.46	−0.46	0.11	0.49	0.57	0.87	0.6	0.33	0.24	−0.11	0.26	0.77	0.2	−0.42	−0.08	−0.28	0.07
TallestStem.9	−0.58	0.5	0.43	0.33	−0.43	0.14	0.71	−0.75	0.14	0.47	0.04	0.21	0.94	−0.1	0.63	−0.21	0.33
TransectCount.9	−0.21	0.34	0.12	0.04	−0.17	−0.51	−0.33	−0.12	0.08	0.27	0.02	−0.79	−0.15	0.71	0.1	0.01	−0.07
Cellulose.8	−0.61	0.63	0.4	0.17	−0.59	−0.23	0.44	−0.87	0.05	0.61	−0.09	−0.12	0.75	0.15	0.89	−0.19	0.53
Hemicellulose.8	−0.27	0.17	−0.31	−0.64	−0.35	−0.23	−0.58	−0.01	−0.22	0.04	−0.23	−0.47	−0.28	0.01	−0.16	0.77	−0.42
Lignin.8	−0.15	0.45	0.24	0.19	−0.22	−0.04	0.37	−0.39	0	0.13	−0.03	0.12	0.44	−0.12	0.5	−0.52	0.81

Fig. 2 Genetic (below diagonal) and phenotypic (above diagonal) correlations among 17 phenotypic traits measured in 138 *Miscanthus sinensis* genotypes. Values on the main diagonal correspond to $\sqrt{H^2}$, where H^2 is the broad-sense heritability of the 17 traits (Table 4).

filtered using our 'stringent' criteria (Table 2), after eliminating one marker from each pair of loci linked at $r^2 \geq 0.8$ (i.e. based on genotypic correlation). Four of the 142 sequenced genotypes were identified as outliers along four different and highly significant axes of variation ($P < 10^{-5}$ from tests based on the Tracy–Widom distribution) based on the default settings of the *smartpca* program within the EIGENSOFT package (Patterson *et al.*, 2006). These genotypes had not been identified as outliers or potential *M. sacchariflorus* hybrids in analyses based on microsatellite and SNP data (Slavov *et al.*, 2013b), and we tentatively assumed that their detection as outliers based on RAD-Seq SNVs was an indication of inferior RAD-Seq data quality. These genotypes were therefore eliminated, and all subsequent analyses were performed using phenotypic and SNV data for the remaining 138 genotypes. However, by performing a subset of analyses based on all 142 genotypes, we also ensured that none of our major results depended on this decision.

Patterns of population structure detected using the PCA approach were also confirmed using the model-based clustering approach implemented in STRUCTURE (Pritchard *et al.*, 2000; Falush *et al.*, 2003, 2007), following the procedure used in a previous study (Slavov *et al.*, 2013b). Briefly, we ran STRUCTURE using the default model parameters and varying the assumed number of genetic groups (*K*) from one to six. Each run consisted of 10 000 burn-in iterations and 10 000 data collection iterations. We used the DISTRUCT program (Rosenberg, 2004) to visualize the results from 10 independent runs that had been aligned using the CLUMPP program (Jakobsson & Rosenberg, 2007). We also used the results from these runs to calculate the *ad hoc* statistic Δ*K*, which tends to peak at the value of *K* that corresponds to the highest hierarchical level of substructure (Evanno *et al.*, 2005), using the online version of the STRUCTURE HARVESTER program (Earl & vonHoldt, 2012). Finally, we used the GCTA program (Yang *et al.*, 2011) to calculate the genetic relationship matrix (Yang *et al.*, 2010) among the 138 genotypes used in all analyses.

GWASs

We used the efficient mixed-model association expedited approach (EMMAX; Kang *et al.*, 2010) to perform GWASs based on SNVs filtered using 'liberal' criteria (Table 2). To control for the confounding effects of cryptic relatedness and population structure, we incorporated the identity-by-state (IBS) kinship matrix (calculated on the basis of all markers using EMMAX) and the first two principal components of population structure (see Sample clustering, population structure and relatedness). This approach is widely used and is believed to provide adequate protection against both environmental and genetic confounding (Price *et al.*, 2010; Vilhjálmsson & Nordborg, 2013). We used data perturbation simulations (Yu *et al.*, 2006) to estimate the statistical power of our EMMAX analyses, as well as to quantify the inflation of naïve estimates of the proportion of variance explained (PVE) by each detected association (Beavis, 1998; Allison *et al.*, 2002; Ingvarsson *et al.*, 2008). For each iteration of the simulations, we randomly chose an SNV from our

© 2013 The Authors
New Phytologist © 2013 New Phytologist Trust

Table 2 Filtering criteria for single-nucleotide variant (SNV) data from 138 *Miscanthus sinensis* genotypes

Filtering criteria	Stringent	Liberal
Q[a]	15	NA
Min depth[b]	14	3
Min ave depth[c]	NA	6
Missing (%)[d]	10	20
Minor alleles[e]	NA	3
Max $\lvert F_{IS}\rvert$[f]	0.25	NA
Min het reads[g]	0.05	NA
No. of alleles[h]	2	2
Statistics		
No. of loci (Sorg)[i]	20 127	53 174
Ave MAF (*Sorg*)[j]	0.027	0.174
Ave $r^2_{1\ kb}$ (*Sorg*)[k]	0.24	0.26
No. of loci (*Misc*)[l]	30 755	121 771
Ave MAF (*Misc*)[m]	0.031	0.115

[a] Q, minimum Phred-like SNV quality score (Li *et al.*, 2008).
[b] *Min depth*, minimum number of reads.
[c] *Min ave depth*, minimum average number of reads across all genotypes.
[d] *Missing* (%), maximum percentage of missing genotype data allowed for a given locus.
[e] *Minor alleles*, minimum number of copies of the minor allele among all genotypes.
[f] *Max* $\lvert F_{IS}\rvert$, maximum deviation of observed genotype frequencies from Hardy–Weinberg expectations, $F_{IS} = 1 - H_o/H_e$, where H_o and H_e are the observed and expected heterozygosities.
[g] *Min het reads*, minimum proportion of reads supporting the less frequent allele in a heterozygous genotype.
[h] *No. of alleles*, number of SNV alleles detected.
[i] *No. of loci* (*Sorg*), number of SNVs that passed all filtering criteria based on alignments to the *Sorghum bicolor* genome.
[j] *Ave MAF* (*Sorg*), average minor allele frequency for SNVs that passed all filtering criteria based on alignments to the *Sorghum bicolor* genome.
[k] *Ave* $r^2_{1\ kb}$ (*Sorg*), average linkage disequilibrium (r^2, calculated as genotypic correlation) for pairs of loci with MAF ≥ 0.10 that aligned within 1 kb of one another in the *Sorghum bicolor* genome.
[l] *No. of loci* (*Misc*), number of SNVs that passed all filtering criteria based on alignments to an *M. sinensis* pseudo-reference.
[m] *Ave MAF* (*Misc*), average minor allele frequency for SNVs that passed all filtering criteria based on alignments to an *M. sinensis* pseudo-reference.
NA, not applicable.

data and assigned constant additive effects $-a$, 0 and a (Falconer, 1989) to genotypes containing 0, 1 and 2 copies, respectively, of an arbitrarily chosen allele (all SNVs used in this study were bi-allelic). These effects were then added to phenotypic trait BLUPs, and the resulting data were analyzed using EMMAX, as described above. This approach preserves the overall structure of the data, whilst also allowing us to estimate statistical power across a range of allele effect sizes, as well as to compare estimated with expected PVE values. The expected value of PVE was calculated as:

$$\mathrm{PVE} = \frac{1}{1 + \frac{1}{2p(1-p)k^2}}, \qquad \text{Eqn 1}$$

where p is the estimated frequency of an arbitrarily chosen SNV allele and k is the simulated additive effect (a) divided by the standard deviation of the respective trait BLUPs (we used *AvgeSen.9*). We chose values of k so that the expected PVE would be between 0.01 and 0.20 in 0.01 increments, and performed 1000 simulations for each of these values. Naïve estimates of PVE were calculated as the R^2 from simple linear regression of the trait BLUP, including simulated additive effects, on SNV genotypes. This was only performed for SNVs that were significantly associated with the simulated trait BLUP at $\alpha = 10^{-5}$.

To assess the relative severity of confounding across traits, we also ran models that only included the IBS kinship matrix, or did not include any terms to account for population structure and relatedness (i.e. simple linear regression of trait BLUP on individual SNVs). In addition, we also used the multi-locus mixed-model (MLMM) approach of Segura *et al.* (2012) to perform a forward–backward model selection procedure and to potentially improve the power, whilst also reducing the rate of false positives of our GWAS analyses. We allowed up to nine forward selection and backward elimination steps and performed the procedure twice, based on MLMMs with or without the first two principal components of population structure included as fixed effects.

Genome-wide prediction

We used the R package rrBLUP (Endelman, 2011) for genome-wide prediction using ridge regression. For a limited subset of analyses, we also used the Bayesian linear regression and the Bayesian LASSO approaches implemented in the BLR package (Perez *et al.*, 2010), but the performance of genome-wide prediction using these approaches was consistently comparable or lower than that using ridge regression, even after including the kinship matrix in the Bayesian models. To assess the effects of varying the size of the training population, we used 2–10-fold random cross-validations (i.e. random allocations of genotypes to training and test populations), which were repeated 100 times for each set of parameters.

Consistent with recommendations on standardizing analytical procedures and benchmarking (Daetwyler *et al.*, 2013), we quantified the performance of genome-wide prediction using three measures. First, we defined predictive ability (r) as Pearson's correlation of BLUPs calculated directly from field data and those obtained from the marker data using ridge regression (Daetwyler *et al.*, 2013). Second, we calculated prediction accuracies (*Accu*) by dividing predictive abilities by the square root of the broad-sense heritability (H) of the respective trait (Legarra *et al.*, 2008). Finally, we also recorded the intercepts (b_0) and slopes (b_1) of the simple linear regressions of BLUPs calculated from field data on those estimated using ridge regression. The last two measures, although not practically meaningful, can be indicative of model deficiencies and/or non-random partitioning of genotypes into training vs test populations (Daetwyler *et al.*, 2013).

To assess the potential of improving the performance of genome-wide prediction by selecting the most informative markers, we compared predictive abilities between cross-validations in which 10, 100, 1000 or 10 000 markers were chosen randomly, based on their GWAS significance (i.e. selecting loci with the lowest GWAS P values) within the training population, or based on their rrBLUP-estimated effects within the training population.

© 2013 The Authors
New Phytologist © 2013 New Phytologist Trust

Results

RAD-Seq genotyping

Our genotyping approach resulted in the detection of over 100 000 putative SNVs (see the Materials and Methods section). A large proportion of these SNVs did not satisfy even our 'liberal' filtering criteria, but even after 'stringent' filtering, over 20 000 informative loci were available for downstream analyses (Table 2). As expected, the chromosome-wide distribution of SNVs appeared to be biased, with very few SNVs detected in putative centromeric regions (Fig. 3). At a finer scale, the vast majority of SNVs detected based on alignments to *Sorghum* (i.e. 98% and 96%, respectively, for 'stringent' and 'liberal' filtering) appeared to be located either inside or within 2 kb of genes.

As expected from the nature of RAD-Seq data, the majority of RAD-Seq SNVs were unlinked. For example, assuming microsynteny between *Sorghum* and *Miscanthus*, we used the sliding window LD-based pruning option of PLINK to calculate that 35 700 of the 53 174 SNVs detected based on alignments to *Sorghum* and 'liberal' filtering had no other SNV within a 25-SNV up- or downstream window that was linked at $r^2 > 0.2$. Similarly, the 121 771 SNVs detected based on alignments to a *Miscanthus* pseudo-reference and 'liberal' filtering were located on 36 223 unique RAD tags. Although our data were not appropriate for detailed estimation of LD and historical rates of recombination (i.e. because of the largely unknown physical distances between SNVs in the *Miscanthus* genome), analyses based on SNVs located on the same RAD tag suggested that fine-scale LD is substantial (average $r^2 = 0.41$ for SNVs with MAF ≥ 0.10, Fig. S1). Furthermore, analyses assuming microsynteny between *Sorghum* and *Miscanthus* clearly demonstrated that significant LD (average $r^2 \geq 0.2$) extends to at least several hundred bp (Table 2) and up to at least 1 Mb for some pairs of SNVs (Fig. S1).

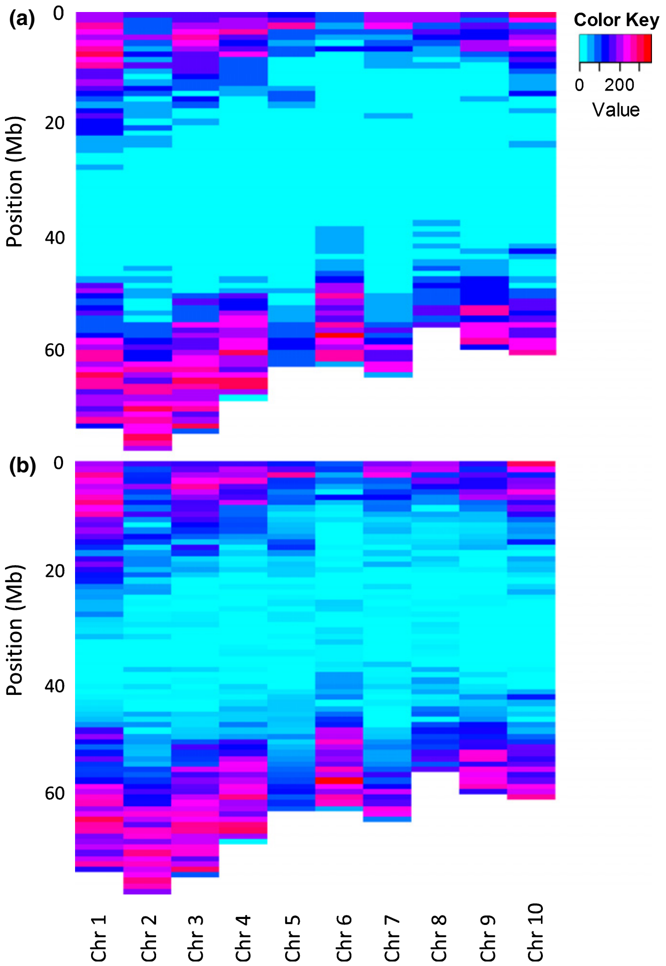

Fig. 3 Chromosome-wide distribution of *Miscanthus sinensis* single-nucleotide variant loci detected based on alignments to *Sorghum bicolor* and filtered using 'stringent' (a) and 'liberal' (b) criteria (Table 2). Each line corresponds to a 1-Mb interval.

Population structure

Individual-based PCA based on SNVs filtered using 'stringent' criteria (Table 2) resulted in the identification of five significant eigenvectors ($P < 10^{-4}$ from tests based on the Tracy–Widom distribution), which explained between 2.9% and 1.2% of the total SNV variation. As expected, PCA (Fig. 1) and model-based clustering (Fig. S2) consistently delineated a 'Continent' vs 'Japan' genetic discontinuity, with both PC1 (Pearson's $|r| = 0.83$, $P < 10^{-15}$) and PC2 (Pearson's $|r| = 0.72$, $P < 10^{-11}$) being strongly correlated with the source longitudes of genotypes with known sampling locations. The differentiation between these two subpopulations was reflected in fine-scale patterns of LD, with r^2 decaying slightly more slowly in each subpopulation than in the overall population (Fig. S1). Furthermore, the clear pattern of clustering based on PC1 and PC2, which accounted for 2.9% and 2.0% of the SNV variation, enabled us to form strong hypotheses about the geographical origins of 68% (47 of 69) of the accessions with unknown sampling locations (Fig. 1).

GWASs

As expected from the relatively small size of our population, data perturbation simulations indicated that GWAS analyses had very limited power to detect associations with small or moderate effects (PVE ≤ 0.10, Fig. S3). When such associations were detected, their estimated effects tended to be upwardly biased by as much as an order of magnitude (Fig. S3).

Naïve GWAS analyses that ignored the effects of population structure and relatedness (i.e. simple linear regression of trait BLUPs on individual SNVs) consistently resulted in severely inflated *P* values (i.e. quantile–quantile (QQ) plots in Figs S4, S5). This effect was particularly strong for traits characterized by strong genetic differentiation (i.e. high Q_{ST} between 'Continent' and 'Japan' subpopulations) and/or significant correlation with geographical variables or primary eigenvectors of population structure (Table 1, Figs S4, S5). The inclusion of the IBS kinship matrix substantially mitigated the confounding for all traits, whereas adding PC1 and PC2 further reduced the inflation of *P* values for some traits (i.e. *BaseDiameter.9*, *LeafWidth.7*, *TransectCount.9*), without apparently compromising statistical

© 2013 The Authors
New Phytologist © 2013 New Phytologist Trust

power relative to models that only included the IBS matrix (Figs S4, S5).

Using this conservative approach (i.e. including both the IBS kinship matrix and PC1 and PC2 as covariates in EMMAX analyses), we detected 35 putative associations ($P < 10^{-5}$) for SNVs resulting from alignments to the *S. bicolor* genome (Fig. S4). Four of these associations (two for *AvgeSen.9*, one for *LeafLength.7* and one for *Lignin.8*) reached genome-wide significance after Bonferroni correction for multiple testing ($P < 0.05/53\,174 \approx 9.4 \times 10^{-7}$), whereas another 13 had an estimated false discovery rate < 0.05 (Table 3). We detected similar patterns using SNVs resulting from alignments to an *M. sinensis* pseudo-reference (Fig. S5), with 53 SNVs reaching suggestive ($P < 10^{-5}$) and two SNVs (one for *DOYFS1.9* and one for *TallestStem.9*) reaching Bonferroni-corrected genome-wide significance ($P < 0.05/121\,771 \approx 4.1 \times 10^{-7}$).

Results from the MLMM-GWAS approach were generally consistent with those from the single-locus EMMAX analyses (Figs S4, S6). However, the MLMM approach allowed us to detect Bonferroni-corrected associations for two additional traits (*BaseDiameter.9* and *TallestStem.9*). Furthermore, when PC1 and PC2 were included as covariates in MLMMs, the selection procedure for *AvgeSen.9* favored a model including six significantly associated SNVs (Fig. S7).

Genome-wide prediction

As expected, predictive abilities were moderately correlated with broad-sense heritabilities (Pearson's $r > 0.57$, $P < 0.018$, Table 4) and appeared to increase monotonically with the size of the training population (Fig. 4a). Although considerable variation was present among the 17 traits, the intercepts and slopes

Table 3 Markers with significant phenotypic associations (false discovery rate < 0.05) in 138 *Miscanthus sinensis* genotypes

Chromosome[a]	Position[b]	P[c]	Q[d]	MAF[e]	PVE[f]	Trait[g]	Gene[h]	Description/annotation
1	3 776 666	3.31E-06	0.03	0.01	0.12	*TallestStem.9*	Sb01g004700	ATVAMP725
1	3 789 996	2.98E-06	0.03	0.02	0.13	*TallestStem.9*	Sb01g004720	Aminoacyl-tRNA synthetase family
1	68 013 320	3.38E-06	0.03	0.01	0.12	*TallestStem.9*	Sb01g044850	Unknown protein
2	67 477 249	1.14E-06	0.03	0.01	0.16	*StatureStemAngle.7*	Sb02g032850	Unknown protein
2	67 477 259	1.14E-06	0.03	0.01	0.16	*StatureStemAngle.7*	Sb02g032850	Unknown protein
3	**8 793 225**	**6.38E-07**[i,j,k]	**0.03**	**0.49**	**0.18**	***LeafLength.7***	**Sb03g008300**	**DNA binding/protein dimerization**
3	**65 293 238**	**2.79E-06**[k]	**0.03**	**0.05**	**0.02**	***AvgeSen.9***	**Sb03g037310**	**ATCDPMEK**
3	65 293 239	2.79E-06	0.03	0.05	0.02	*AvgeSen.9*	Sb03g037310	ATCDPMEK
4	4 150 586	1.57E-06	0.04	0.06	0.18	*LeafLength.7*	NA	NA
6	50 249 485	3.35E-06	0.03	0.02	0.16	*TallestStem.9*	Sb06g020830	Protein kinase family protein
6	**54 211 630**	**8.64E-07**[i,j,k]	**0.05**	**0.17**	**0.15**	***Lignin.8***	**Sb06g025250**	**Serine-type endopeptidase/serine-type peptidase**
6	**58 247 799**	**5.66E-07**[i,j]	**0.02**	**0.03**	**0.25**	***AvgeSen.9***	**Sb06g029670**	**ATP binding/protein kinase/protein serine/threonine kinase/protein tyrosine kinase/sugar binding**
9	24 591 741	1.84E-06	0.03	0.03	0.26	*AvgeSen.9*	NA	NA
9	46 480 666	4.07E-06	0.04	0.15	0.02	*AvgeSen.9*	Sb09g018620	Hydroxyproline-rich glycoprotein family protein
10	**49 962 793**	**4.90E-07**[i,k]	**0.02**	**0.04**	**0.21**	***AvgeSen.9***	**Sb10g022360**	**Unknown protein**
10	**55 336 585**	**3.14E-06**[j]	**0.03**	**0.01**	**0.12**	***TallestStem.9***	**Sb10g026010**	**UBP19; cysteine-type endopeptidase/ubiquitin thiolesterase**
10	**59 574 096**	**1.50E-06**[j]	**0.03**	**0.05**	**0.19**	***TallestStem.9***	**Sb10g029835**	**Unknown protein**

Associations with Bonferroni-corrected genome-wide significance ($\alpha = 0.05$) are shown in bold. Only results for markers detected from alignments to the *Sorghum bicolor* genome are shown.

[a] Chromosome, *Sorghum bicolor* chromosome to which the marker was aligned.

[b] Position, *Sorghum bicolor* chromosome position to which the marker was aligned.

[c] *P*, *P* value from genome-wide association studies (GWAS) analysis using the efficient mixed-model association expedited approach (EMMAX), including the kinship matrix and the first two eigenvectors of population structure (see the Materials and Methods section).

[d] Q, false discovery rate calculated using the *q*-value R package (Dabney & Storey, 2013).

[e] MAF, minor allele frequency.

[f] PVE, naïve estimate of the proportion of variance explained based on simple linear regression (see the Materials and Methods section).

[g] Trait, phenotypic trait as defined in Table 1.

[h] Gene, *Sorghum bicolor* gene to which the marker was aligned.

[i] Significant at genome-wide $\alpha = 0.05$ after Bonferroni correction based on EMMAX analyses (see the Materials and Methods section).

[j] Included in the optimal model according to the multiple Bonferroni criterion in multi-locus mixed-model (MLMM) analyses (see the Materials and Methods section).

[k] Included in the optimal model according to the multiple Bonferroni criterion in MLMM analyses including the first two eigenvectors of population structure (see the Materials and Methods section).

NA, not applicable (markers aligning to putatively intergenic positions).

© 2013 The Authors
New Phytologist © 2013 New Phytologist Trust

Table 4 Performance of genome-wide prediction in 138 *Miscanthus sinensis* genotypes based on single-nucleotide variant (SNV) markers filtered using liberal criteria (Table 2)

Trait[a]	H^{2b}	r_{Sorg} (SD)[c]	$Accu_{Sorg}$ (SD)[d]	r_{Misc} (SD)[e]	$Accu_{Misc}$ (SD)[f]
Phenology					
DOYFS1.9	0.89	0.76 (0.02)	0.81 (0.02)	0.78 (0.01)	0.82 (0.02)
AvgeSen.9	0.83	0.64 (0.01)	0.71 (0.01)	0.64 (0.01)	0.71 (0.01)
Morphology/biomass					
BaseDiameter.9	0.52	0.27 (0.05)	0.38 (0.06)	0.29 (0.04)	0.40 (0.06)
DryMatter.9	0.54	0.06 (0.05)	0.09 (0.07)	0.04 (0.06)	0.05 (0.08)
LeafLength.7	0.65	0.67 (0.01)	0.83 (0.01)	0.66 (0.01)	0.82 (0.01)
LeafWidth.7	0.64	0.52 (0.02)	0.65 (0.03)	0.56 (0.01)	0.70 (0.02)
MaxCanopyHeight.9	0.77	0.35 (0.03)	0.40 (0.03)	0.34 (0.02)	0.39 (0.03)
Moisture.9	0.59	0.70 (0.01)	0.92 (0.01)	0.73 (0.01)	0.95 (0.01)
StatureCategory.7	0.48	0.39 (0.03)	0.57 (0.04)	0.43 (0.02)	0.62 (0.03)
StatureLeafAngle.7	0.50	0.46 (0.03)	0.65 (0.05)	0.47 (0.02)	0.66 (0.03)
StatureStemAngle.7	0.48	0.37 (0.02)	0.53 (0.03)	0.40 (0.02)	0.58 (0.03)
StemDiameter.9	0.60	0.51 (0.03)	0.66 (0.04)	0.50 (0.02)	0.65 (0.03)
TallestStem.9	0.88	0.65 (0.01)	0.69 (0.01)	0.63 (0.01)	0.68 (0.02)
TransectCount.9	0.51	0.17 (0.04)	0.23 (0.06)	0.27 (0.03)	0.39 (0.04)
Cell wall composition					
Cellulose.8	0.79	0.62 (0.02)	0.70 (0.02)	0.61 (0.02)	0.69 (0.02)
Hemicellulose.8	0.60	0.25 (0.03)	0.32 (0.04)	0.18 (0.04)	0.24 (0.05)
Lignin.8	0.66	0.43 (0.02)	0.53 (0.03)	0.35 (0.02)	0.43 (0.03)
Average (SD)[g]	0.64	0.46 (0.20)	0.57 (0.22)	0.46 (0.20)	0.57 (0.23)

All predictive abilities and accuracies are based on 100 random 10-fold cross-validations (i.e. using a training population with $N = 124$ genotypes).

[a] Trait, phenotypic trait as defined in Table 1.

[b] H^2, broad-sense heritability (see the Materials and Methods section).

[c] r_{Sorg} (SD), average predictive ability and standard deviation across 100 random 10-fold cross-validations based on 53 174 SNVs obtained from alignments to the *Sorghum bicolor* genome.

[d] $Accu_{Sorg}$ (SD), average accuracy of genome-wide prediction and standard deviation across 100 random 10-fold cross-validations based on 53 174 SNVs obtained from alignments to the *S. bicolor* genome

[e] r_{Misc} (SD), average predictive ability and standard deviation across 100 random 10-fold cross-validations based on 121 771 SNVs obtained from alignments to an *M. sinensis* pseudo-reference.

[f] $Accu_{Misc}$ (SD), average accuracy of genome-wide prediction and standard deviation across 100 random 10-fold cross-validations based on 121 771 SNVs obtained from alignments to an *M. sinensis* pseudo-reference.

[g] Average (SD), overall average and standard deviation across traits.

of simple linear regressions of BLUPs calculated from field data on those estimated using ridge regression tended to be close to their expected values of 0.00 and 1.00, respectively (Table S1). Interestingly, both predictive abilities and accuracies of genome-wide prediction were statistically indistinguishable ($P > 0.64$ from paired *t*-tests across traits) between the sets of SNVs obtained based on different alignments (Table 4). Furthermore, predictive abilities tended to reach a plateau when *c.* 10 000–20 000 markers were used (i.e. approximately half of the *c.* 35 000–36 000 presumably independent loci), with further increases resulting in little or no improvement (Fig. 4b). Genetic structure (Fig. 1) and the presence of closely related genotypes in the training and test populations (Fig. S8) affected the performance of genome-wide prediction, with predictive abilities from cross-validations across subpopulations being significantly lower than those from corresponding random cross-validations (one-sided $P = 0.0004$ from a paired *t*-test across traits). However, the extent of this difference varied considerably among traits (Fig. 5). Finally, the selection of markers based on their GWAS significance or rrBLUP-estimated effects appears to have potential for improving predictive abilities (Fig. 6), particularly for traits with lower heritabilities (Fig. 6b).

Discussion

As in a number of previous studies across a wide phylogenetic range of plant species (Barchi *et al.*, 2011; Chutimanitsakun *et al.*, 2011; Stölting *et al.*, 2013), the application of RAD-Seq genotyping resulted in the generation of large numbers of informative SNV markers (Table 2). Alignments of RAD tags to an *M. sinensis* pseudo-reference resulted in the identification of substantially greater numbers of markers (Table 2) and indistinguishable performance of genome-wide prediction (Table 4) compared with alignments to the *S. bicolor* genome. However, it is possible that the availability of a reference genome sequence from a closer relative would have resulted in more informative RAD-Seq SNV data. In any case, our results indicate that the *a priori* availability of a high-quality reference genome sequence does not appear to be a requirement for the success of this genotyping procedure.

Although we were able to generate data for a large number of RAD-Seq markers, the use of a methylation-sensitive enzyme (*Pst*I) and relatively stringent alignment criteria resulted in a greatly unbalanced genome coverage (Fig. 3) and strong bias against intergenic SNVs. Although probably advantageous in

© 2013 The Authors
New Phytologist © 2013 New Phytologist Trust

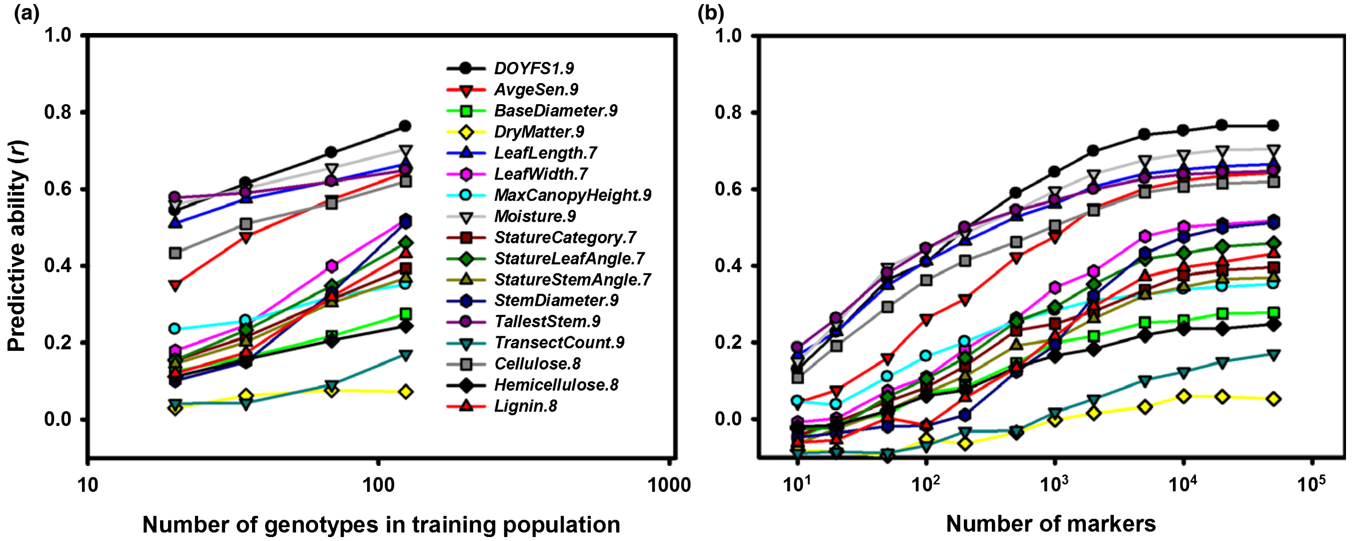

Fig. 4 Performance of genome-wide prediction in a population of 138 *Miscanthus sinensis* genotypes using single-nucleotide variant markers obtained from alignments to the *Sorghum bicolor* genome. Predictive ability as a function of training population size (a) and number of markers used (b). All data points are averages across 100 random cross-validations.

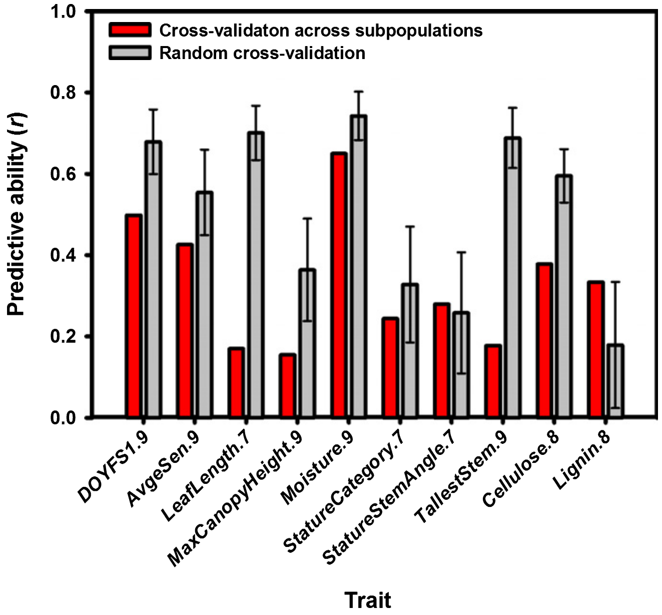

Fig. 5 Effect of population structure on the performance of genome-wide prediction in a population of 70 *Miscanthus sinensis* genotypes with known sampling locations using single-nucleotide variants obtained from alignments to the *Sorghum bicolor* genome. Cross-validations across subpopulations (red bars) were performed using genotypes from Japan ($N = 43$) as a training population and genotypes from China and South Korea ($N = 27$) as a test population. Random cross-validations (gray bars) were performed by randomly selecting the same numbers of genotypes in the training and test populations from the total set of 138 genotypes. All data points are averages, and error bars correspond to standard deviations across 100 random cross-validations. Only traits with cross-subpopulation predictive abilities exceeding (1) 0.10 and (2) the standard deviation from the random cross-validations for the respective trait are shown.

terms of data quality, this effect may limit the applicability of RAD-Seq genotyping for the complete dissection of complex trait architecture because over half of trait-associated polymorphisms may be located outside of genes (Li *et al*., 2012). However, this shortcoming could possibly be mitigated by using multiple restriction enzymes with varying sensitivities to methylation.

The patterns of putatively neutral population structure detected based on RAD-Seq SNVs (Fig. 1) were consistent with those described previously based on much smaller numbers of markers (Slavov *et al*., 2013b). However, the greater power of the RAD-Seq markers allowed us to detect additional nuances, as well as to form hypotheses about the geographical origins of over two-thirds of the genotypes with unknown sampling locations (Fig. 1). Extensions of this approach to wider germplasm collections (including other *Miscanthus* species) and more sophisticated models (Baran *et al*., 2013) will significantly improve our knowledge about the evolutionary history of the genus and will provide important practical information to breeders.

Despite the small size of our association mapping population ($N = 138$), seven associations consistently reached genome-wide significance across a range of GWAS analyses and adjustments for multiple testing (Table 3, Figs S4–S7). Interestingly, two of these associations (i.e. one for *AvgeSen.9* and one for *Lignin.8*; Table 3), as well as another two putative associations for *StemDiameter.9* and *TallestStem.9* ($P < 10^{-5}$, Fig. S4), all appeared to align within 8–16 Mb of the putative dwarfing locus *dw2*, whose location was recently supported by a GWAS for plant height in *S. bicolor* (Morris *et al*., 2013). This region may therefore require particular attention in future association and linkage mapping studies.

What is the explanation for the detection of multiple significant associations, given the relatively limited statistical power of our GWASs (Fig. S3)? Because no single unambiguous explanation can be provided, we hypothesize that several factors may underlie this observation. First, LD in *M. sinensis* (Fig. S1) does not appear to be as extensive as in its primarily self-pollinating

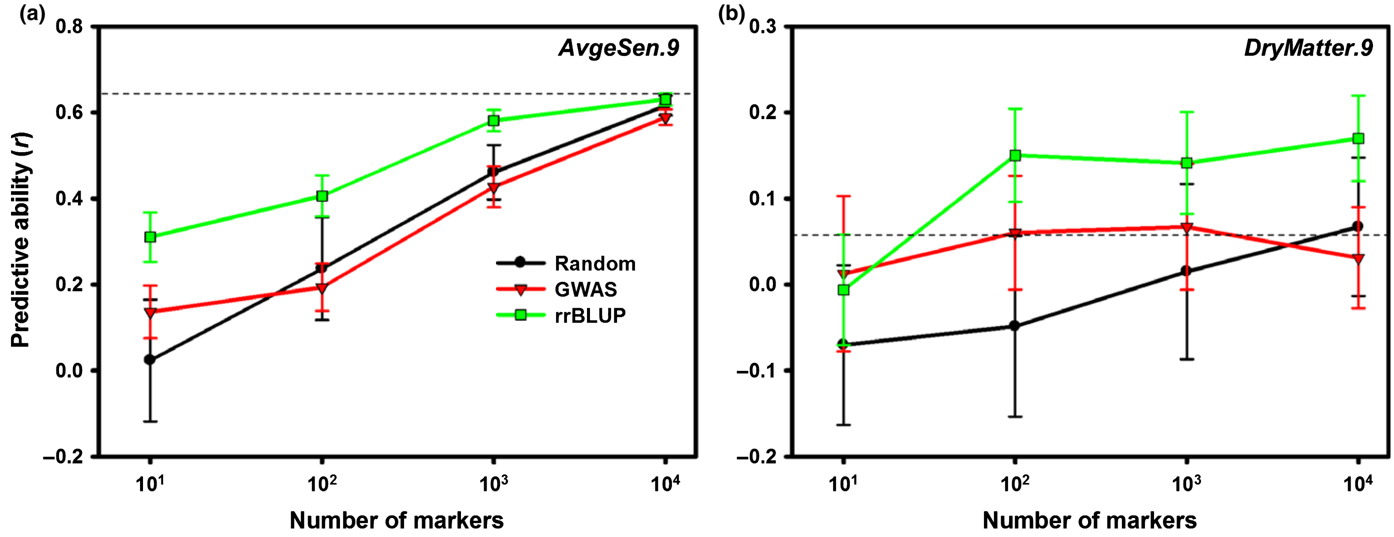

Fig. 6 Effect of marker selection on the performance of genome-wide prediction of average senescence score (a) and total dry weight (b) in a population of 138 *Miscanthus sinensis* genotypes based on single-nucleotide variants (SNVs) detected from alignments to the *Sorghum bicolor* genome. 'Random' (circles, black line), randomly selected markers; 'GWAS' (triangles, red line), markers with the lowest genome-wide association study *P* values within the training population; 'rrBLUP' (squares, green line), markers with the highest estimated effects within the training population based on ridge regression. All data points are averages ± SD across 100 random cross-validations. Dashed lines correspond to predictive abilities based on all 53 174 SNVs.

relative *S. bicolor* (Morris *et al.*, 2013). However, there was clear evidence of long-range LD in at least some regions of the *M. sinensis* genome (Fig. S1). Thus, although the initial stages of follow-up studies will focus on the regions in the immediate vicinity of trait-associated SNVs, it is conceivable that at least some of these are tagging causative polymorphisms located many kilobases away. Second, the statistical power to detect associations of small to moderate effect (PVE ≤ 0.10) was only between 0.001 and 0.213 (Fig. S3). However, if the genomic architectures of the traits that we studied are highly complex, dozens or even hundreds of causative polymorphisms with minor effects may exist across the genome. Under this highly polygenic scenario, even an underpowered study that uses a large number of markers is likely to detect a subset of minor effect associations and dramatically overestimate their PVE (Fig. S3). Alternatively, some of the SNVs detected by our GWASs may be linked to causative polymorphisms of larger effects. However, the former scenario seems to be more plausible based on larger scale GWAS results in other related crops (Buckler *et al.*, 2009; Morris *et al.*, 2013). Furthermore, the highly polygenic scenario is consistent with the results from our assessment of marker selection strategies for genome-wide prediction (Fig. 6), which was performed through cross-validation and should therefore be immune to the inflation of effect sizes. Finally, it is possible that our analytical procedures failed to control the rate of false positives. However, our results (i.e. QQ plots in Figs S4, S5) are generally inconsistent with this explanation.

Although GWAS results are expected to improve in the near future (i.e. with the use of larger populations and denser genome coverage), the ability to predict phenotypes from a genome-wide set of markers is likely to have immediate impact on *Miscanthus* breeding programs. Our genome-wide prediction results illustrate several important points. First, as expected from both theoretical and empirical studies (Daetwyler *et al.*, 2008, 2010, 2013; Resende *et al.*, 2012), trait heritability was correlated with predictive ability. However, this correlation was only moderate, confirming that other factors (e.g. genomic architecture of the trait, LD, effective population size) may be equally important (Daetwyler *et al.*, 2010; de Los Campos *et al.*, 2013). For example, *DryMatter.9* was moderately heritable ($H^2 = 0.54$), yet genome-wide prediction of this trait consistently failed (Table 4, Fig. 4). This is not surprising, given the highly composite nature of biomass yield, and targeting individual yield components or correlates (e.g. *MaxCanopyHeight.9* and *StemDiameter.9*; Fig. 2) appears to be a more promising approach (Table 4, Fig. 4). In contrast, the accuracy of genome-wide prediction for *Moisture.9* ($H^2 = 0.59$) nearly reached its theoretical maximum (Table 4), suggesting that genomic selection for this trait may be feasible even with very small training populations (i.e. $N < 100$, Fig. 4a), with as few as 100–1000 markers (Fig. 4b) and across subpopulations (Fig. 5). Predictive ability was similarly high for phenological traits (i.e. *DOYFS1.9* and *AvgeSen.9*), as well as *Cellulose.8*, and promising for most other traits (i.e. except *DryMatter.9* and *TransectCount.9*; Table 4, Fig. 4). We are therefore exploring the practical application and validation of genomic selection in the *Miscanthus* breeding program at the Institute of Biological, Environmental and Rural Sciences (IBERS). Second, our results clearly suggest that substantial further improvements in predictive ability are more likely to come from using larger training populations (Fig. 4a) than from using denser genome coverage (Fig. 4b). However, an important caveat is that the SNVs that we used probably did not cover vast regions of the *Miscanthus* genome (Fig. 3). The observed plateau in predictive ability when 10 000–20 000 SNVs were used clearly needs to be validated using more representative samples of markers. However, based on our results and currently available genotyping platforms, our

© 2013 The Authors
New Phytologist © 2013 New Phytologist Trust

recommended approach to genome-wide prediction in non-model plants would be to maximize the number of individuals in the training population and to use a low-cost genotyping strategy (Davey *et al.*, 2011; Elshire *et al.*, 2011; Poland *et al.*, 2012). Third, the robustness of genome-wide prediction across subpopulations varied dramatically among traits (Fig. 5). Thus, the relationship between training and test populations needs to be characterized in detail, and individuals from the populations targeted by genomic selection (or their close relatives) should ideally be included in training populations. Finally, our preliminary assessment of locus selection strategies (Fig. 6) clearly indicated that there is great potential to increase predictive abilities through the application of sophisticated analytical approaches (de Los Campos *et al.*, 2013), which do not attempt to estimate phenotypic effects for all loci (i.e. in contrast to the method we used). The refinement of these approaches and their combination with multi-locus and multi-trait procedures (Korte *et al.*, 2012; Segura *et al.*, 2012) offer exciting prospects for the characterization of pleiotropy and the dissection of highly complex phenotypic traits. However, studies aimed at pushing the limits of genome-wide prediction cannot overcome the inherent limitations of this approach (e.g. trait heritability sets an upper limit on accuracy) and need to be designed and interpreted with awareness of its numerous pitfalls (Wray *et al.*, 2013).

In summary, we related high-quality phenotypic data for 17 traits in a population of *M. sinensis* to SNV markers obtained through RAD-Seq genotyping. Despite the relatively small size of our experimental population ($N = 138$), results from GWASs were promising and suggest that this approach will be instrumental for the dissection of complex phenotypic traits. On a more immediate time-scale, results from our genome-wide prediction analyses suggest that the application of genomic selection in *Miscanthus* may be feasible, and we are therefore validating this finding in our accelerated breeding program.

Acknowledgements

G.S. was funded by the Biosciences, Environment and Agriculture Alliance whilst working on the manuscript. Funding was also provided by the UK Biotechnology and Biological Sciences Research Council (BBSRC) Institute Strategic Programme grant BB/J0042/1 and by BBSRC responsive mode grant BB/K01711X/1. We thank the Editor and three anonymous reviewers for their comments on an earlier version of the manuscript, as well as John Norris for providing Linux computing support.

References

Allison DB, Fernandez JR, Heo M, Zhu SK, Etzel C, Beasley TM, Amos CI. 2002. Bias in estimates of quantitative-trait-locus effect in genome scans: demonstration of the phenomenon and a method-of-moments procedure for reducing bias. *American Journal of Human Genetics* **70**: 575–585.

Allison GG, Morris C, Clifton-Brown J, Lister SJ, Donnison IS. 2011. Genotypic variation in cell wall composition in a diverse set of 244 accessions of *Miscanthus*. *Biomass and Bioenergy* **35**: 4740–4747.

Baird NA, Etter PD, Atwood TS, Currey MC, Shiver AL, Lewis ZA, Selker EU, Cresko WA, Johnson EA. 2008. Rapid SNP discovery and genetic mapping using sequenced RAD markers. *PLoS One* **3**: e3376.

Baran Y, Quintela I, Carracedo A, Pasaniuc B, Haperin E. 2013. Enhanced localization of genetic samples through linkage-disequilibrium correction. *American Journal of Human Genetics* **92**: 882–894.

Barchi L, Lanteri S, Portis E, Acquadro A, Vale G, Toppino L, Rotino GL. 2011. Identification of SNP and SSR markers in eggplant using RAD tag sequencing. *BMC Genomics* **12**: 304.

Beavis WD. 1998. QTL analyses: power, precision, and accuracy. In: Paterson AH, ed. *Molecular dissection of complex traits*. Boca Raton, FL, USA: CRC Press, 145–162.

Buckler ES, Holland JB, Bradbury PJ, Acharya CB, Brown PJ, Browne C, Ersoz E, Flint-Garcia S, Garcia A, Glaubitz JC *et al.* 2009. The genetic architecture of maize flowering time. *Science* **325**: 714–718.

Cardon LR, Bell JI. 2001. Association study designs for complex diseases. *Nature Reviews Genetics* **2**: 91–99.

Chutimanitsakun Y, Nipper RW, Cuesta-Marcos A, Cistue L, Corey A, Filichkina T, Johnson EA, Hayes PM. 2011. Construction and application for QTL analysis of a Restriction Site Associated DNA (RAD) linkage map in barley. *BMC Genomics* **12**: 4.

Clifton-Brown JC, Breuer J, Jones MB. 2007. Carbon mitigation by the energy crop, *Miscanthus*. *Global Change Biology* **13**: 2296–2307.

Clifton-Brown JC, Stampfl PF, Jones MB. 2004. *Miscanthus* biomass production for energy in Europe and its potential contribution to decreasing fossil fuel carbon emissions. *Global Change Biology* **10**: 509–518.

Dabney A, Storey JD. 2013. *qvalue: Q-value estimation for false discovery rate control. R package version 1.34.0*. URL: http://www.bioconductor.org/packages/release/bioc/html/qvalue.html.

Daetwyler HD, Calus MPL, Pong-Wong R, de Los Campos G, Hickey JM. 2013. Genomic prediction in animals and plants: simulation of data, validation, reporting, and benchmarking. *Genetics* **193**: 347–365.

Daetwyler HD, Pong-Wong R, Villanueva B, Woolliams JA. 2010. The impact of genetic architecture on genome-wide evaluation methods. *Genetics* **185**: 1021–1031.

Daetwyler HD, Villanueva B, Woolliams JA. 2008. Accuracy of predicting the genetic risk of disease using a genome-wide approach. *PLoS One* **3**: e3395.

Danecek P, Auton A, Abecasis G, Albers CA, Banks E, DePristo MA, Handsaker RE, Lunter G, Marth GT, Sherry ST *et al.* 2011. The variant call format and VCFtools. *Bioinformatics* **27**: 2156–2158.

Davey JW, Hohenlohe PA, Etter PD, Boone JQ, Catchen JM, Blaxter ML. 2011. Genome-wide genetic marker discovery and genotyping using next-generation sequencing. *Nature Reviews Genetics* **12**: 499–510.

Earl D, vonHoldt B. 2012. STRUCTURE HARVESTER: a website and program for visualizing STRUCTURE output and implementing the Evanno method. *Conservation Genetics Resources* **4**: 359–361.

Elshire RJ, Glaubitz JC, Sun Q, Poland JA, Kawamoto K, Buckler ES, Mitchell SE. 2011. A robust, simple genotyping-by-sequencing (GBS) approach for high diversity species. *PLoS One* **6**: e19379.

Endelman JB. 2011. Ridge regression and other kernels for genomic selection with R package rrBLUP. *Plant Genome* **4**: 250–255.

Evanno G, Regnaut S, Goudet J. 2005. Detecting the number of clusters of individuals using the software STRUCTURE: a simulation study. *Molecular Ecology* **14**: 2611–2620.

Falconer DS. 1989. *Introduction to quantitative genetics*. Harlow, UK: Longman.

Falush D, Stephens M, Pritchard JK. 2003. Inference of population structure using multilocus genotype data: linked loci and correlated allele frequencies. *Genetics* **164**: 1567–1587.

Falush D, Stephens M, Pritchard JK. 2007. Inference of population structure using multilocus genotype data: dominant markers and null alleles. *Molecular Ecology Notes* **7**: 574–578.

Feltus FA, Vandenbrink JP. 2012. Bioenergy grass feedstock: current options and prospects for trait improvement using emerging genetic, genomic, and systems biology toolkits. *Biotechnology for Biofuels* **5**: 80.

© 2013 The Authors
New Phytologist © 2013 New Phytologist Trust

Foley JA, Ramankutty N, Brauman KA, Cassidy ES, Gerber JS, Johnston M, Mueller ND, O'Connell C, Ray DK, West PC *et al.* 2011. Solutions for a cultivated planet. *Nature* **478**: 337–342.

Hamblin MT, Buckler ES, Jannink JL. 2011. Population genetics of genomics-based crop improvement methods. *Trends in Genetics* **27**: 98–106.

Hastings A, Clifton-Brown J, Wattenbach M, Mitchell CP, Stampfl P, Smith P. 2009. Future energy potential of *Miscanthus* in Europe. *Global Change Biology Bioenergy* **1**: 180–196.

Howe GT, Saruul P, Davis J, Chen THH. 2000. Quantitative genetics of bud phenology, frost damage, and winter survival in an F2 family of hybrid poplars. *Theoretical and Applied Genetics* **101**: 632–642.

Ingvarsson PK, Garcia MV, Luquez V, Hall D, Jansson S. 2008. Nucleotide polymorphism and phenotypic associations within and around the phytochrome B2 locus in European aspen (*Populus tremula*, Salicaceae). *Genetics* **178**: 2217–2226.

Jakobsson M, Rosenberg NA. 2007. CLUMPP: a cluster matching and permutation program for dealing with label switching and multimodality in analysis of population structure. *Bioinformatics* **23**: 1801–1806.

Jensen E, Farrar K, Thomas-Jones S, Hastings A, Donnison I, Clifton-Brown J. 2011. Characterization of flowering time diversity in *Miscanthus* species. *Global Change Biology Bioenergy* **3**: 387–400.

Kang HM, Sul JH, Service SK, Zaitlen NA, Kong SY, Freimer NB, Sabatti C, Eskin E. 2010. Variance component model to account for sample structure in genome-wide association studies. *Nature Genetics* **42**: 348–354.

Korte A, Vilhjálmsson BJ, Segura V, Platt A, Long Q, Nordborg M. 2012. A mixed-model approach for genome-wide association studies of correlated traits in structured populations. *Nature Genetics* **44**: 1066–1071.

Langmead B, Trapnell C, Pop M, Salzberg SL. 2009. Ultrafast and memory-efficient alignment of short DNA sequences to the human genome. *Genome Biology* **10**: R25.

Legarra A, Robert-Granie C, Manfredi E, Elsen J-M. 2008. Performance of genomic selection in mice. *Genetics* **180**: 611–618.

Li H, Handsaker B, Wysoker A, Fennell T, Ruan J, Homer N, Marth G, Abecasis G, Durbin R. 2009. The sequence alignment/map format and SAMtools. *Bioinformatics* **25**: 2078–2079.

Li H, Ruan J, Durbin R. 2008. Mapping short DNA sequencing reads and calling variants using mapping quality scores. *Genome Research* **18**: 1851–1858.

Li X, Zhu C, Yeh CT, Wu W, Takacs EM, Petsch KA, Tian F, Bai G, Buckler ES, Muehlbauer GJ *et al.* 2012. Genic and nongenic contributions to natural variation of quantitative traits in maize. *Genome Research* **22**: 2436–2444.

de Los Campos G, Hickey JM, Pong-Wong R, Daetwyler HD, Calus MPL. 2013. Whole-genome regression and prediction methods applied to plant and animal breeding. *Genetics* **193**: 327–345.

Meuwissen THE, Hayes BJ, Goddard ME. 2001. Prediction of total genetic value using genome-wide dense marker maps. *Genetics* **157**: 1819–1829.

Morrell PL, Buckler ES, Ross-Ibarra J. 2012. Crop genomics: advances and applications. *Nature Reviews Genetics* **13**: 85–96.

Morris GP, Ramu P, Deshpande SP, Hash CT, Shah T, Upadhyaya HD, Riera-Lizarazu O, Brown PJ, Acharya CB, Mitchell SE *et al.* 2013. Population genomic and genome-wide association studies of agroclimatic traits in sorghum. *Proceedings of the National Academy of Sciences, USA* **110**: 453–458.

Paterson AH, Bowers JE, Bruggmann R, Dubchak I, Grimwood J, Gundlach H, Haberer G, Hellsten U, Mitros T, Poliakov A *et al.* 2009. The *Sorghum bicolor* genome and the diversification of grasses. *Nature* **457**: 551–556.

Patterson N, Price AL, Reich D. 2006. Population structure and eigenanalysis. *PLoS Genetics* **2**: 2074–2093.

Perez P, de los Campos G, Crossa J, Gianola D. 2010. Genomic-enabled prediction based on molecular markers and pedigree using the Bayesian linear regression package in R. *Plant Genome* **3**: 106–116.

Poland JA, Brown PJ, Sorrells ME, Jannink JL. 2012. Development of high-density genetic maps for barley and wheat using a novel two-enzyme genotyping-by-sequencing approach. *PLoS One* **7**: e32253.

Price AL, Zaitlen NA, Reich D, Patterson N. 2010. New approaches to population stratification in genome-wide association studies. *Nature Reviews Genetics* **11**: 459–463.

Pritchard JK, Stephens M, Donnelly P. 2000. Inference of population structure using multilocus genotype data. *Genetics* **155**: 945–959.

Purcell S, Neale B, Todd-Brown K, Thomas L, Ferreira MAR, Bender D, Maller J, Sklar P, de Bakker PIW, Daly MJ *et al.* 2007. PLINK: a tool set for whole-genome association and population-based linkage analyses. *American Journal of Human Genetics* **81**: 559–575.

Resende MFR Jr, Munoz P, Resende MDV, Garrick DJ, Fernando RL, Davis JM, Jokela EJ, Martin TA, Peter GF, Kirst M. 2012. Accuracy of genomic selection methods in a standard data set of loblolly pine (*Pinus taeda* L.). *Genetics* **190**: 1503–1510.

Robson P, Mos M, Clifton-Brown J, Donnison I. 2012. Phenotypic variation in senescence in *Miscanthus*: towards optimising biomass quality and quantity. *Bioenergy Research* **5**: 95–105.

Rosenberg NA. 2004. DISTRUCT: a program for the graphical display of population structure. *Molecular Ecology Notes* **4**: 137–138.

Rubin EM. 2008. Genomics of cellulosic biofuels. *Nature* **454**: 841–845.

Segura V, Vilhjálmsson BJ, Platt A, Korte A, Seren U, Long Q, Nordborg M. 2012. An efficient multi-locus mixed-model approach for genome-wide association studies in structured populations. *Nature Genetics* **44**: 825–830.

Service RF. 2013. Battle for the barrel. *Science* **339**: 1374–1379.

Sims RE, Mabee W, Saddler JN, Taylor M. 2010. An overview of second generation biofuel technologies. *Bioresource Technology* **101**: 1570–1580.

Slavov GT, Allison GG, Bosch M. 2013a. Advances in the genetic dissection of plant cell walls: tools and resources available in *Miscanthus*. *Frontiers in Plant Science* **4**: 217.

Slavov GT, Robson P, Jensen E, Hodgson E, Farrar K, Allison GG, Hawkins S, Thomas-Jones S, Ma XF, Huang L *et al.* 2013b. Contrasting geographic patterns of genetic variation for molecular markers vs phenotypic traits in the energy grass *Miscanthus sinensis*. *Global Change Biology Bioenergy* **5**: 562–571.

Stölting KN, Nipper R, Lindtke D, Caseys C, Waeber S, Castiglione S, Lexer C. 2013. Genomic scan for single nucleotide polymorphisms reveals patterns of divergence and gene flow between ecologically divergent species. *Molecular Ecology* **22**: 842–855.

Valentine J, Clifton-Brown J, Hastings A, Robson P, Allison G, Smith P. 2012. Food vs. fuel: the use of land for lignocellulosic next generation energy crops that minimize competition with primary food production. *Global Change Biology Bioenergy* **4**: 1–19.

Vilhjálmsson BJ, Nordborg M. 2013. The nature of confounding in genome-wide association studies. *Nature Reviews Genetics* **14**: 1–2.

Wray NR, Yang J, Hayes BJ, Price AL, Goddard ME, Visscher PM. 2013. Pitfalls of predicting complex traits from SNPs. *Nature Reviews Genetics* **14**: 507–515.

Yang J, Lee SH, Goddard ME, Visscher PM. 2011. GCTA: a tool for genome-wide complex trait analysis. *American Journal of Human Genetics* **88**: 76–82.

Yang JA, Benyamin B, McEvoy BP, Gordon S, Henders AK, Nyholt DR, Madden PA, Heath AC, Martin NG, Montgomery GW *et al.* 2010. Common SNPs explain a large proportion of the heritability for human height. *Nature Genetics* **42**: 565–569.

Yu JM, Pressoir G, Briggs WH, Bi IV, Yamasaki M, Doebley JF, McMullen MD, Gaut BS, Nielsen DM, Holland JB *et al.* 2006. A unified mixed-model method for association mapping that accounts for multiple levels of relatedness. *Nature Genetics* **38**: 203–208.

Supporting Information

Additional supporting information may be found in the online version of this article.

Fig. S1 Linkage disequilibrium based on single-nucleotide variants detected using restriction site-associated DNA sequencing in *Miscanthus sinensis.*

Fig. S2 Model-based clustering of single-nucleotide variant data for 138 *Miscanthus sinensis* genotypes.

© 2013 The Authors
New Phytologist © 2013 New Phytologist Trust

Fig. S3 Statistical power and effect size inflation based on data perturbation simulations for genome-wide association study analyses using the EMMAX program.

Fig. S4 Genome-wide association study (GWAS) results for 17 phenotypic traits in a population of 138 *Miscanthus sinensis* genotypes based on 53 174 markers detected using alignments to the *Sorghum bicolor* genome.

Fig. S5 Genome-wide association study (GWAS) results for 17 phenotypic traits in a population of 138 *Miscanthus sinensis* genotypes based on 121 771 markers detected using alignments to a *M. sinensis* pseudo-reference.

Fig. S6 Multi-locus mixed-model (MLMM) genome-wide association study results for 17 phenotypic traits in a population of 138 *Miscanthus sinensis* genotypes based on 53 174 markers detected using alignments to the *Sorghum bicolor* genome.

Fig. S7 Covariate multi-locus mixed-model (MLMM) genome-wide association study (GWAS) results for average senescence score in a population of 138 *Miscanthus sinensis* genotypes based on 53 174 markers detected using alignments to the *Sorghum bicolor* genome.

Fig. S8 Genetic relationship matrix among 138 *Miscanthus sinensis* genotypes.

Table S1 Simple linear regression measures of performance of genome-wide prediction in a population of 138 *Miscanthus sinensis* genotypes

Methods S1 *Miscanthus* pseudo-reference.

Please note: Wiley Blackwell are not responsible for the content or functionality of any supporting information supplied by the authors. Any queries (other than missing material) should be directed to the *New Phytologist* Central Office.

About *New Phytologist*

- *New Phytologist* is an electronic (online-only) journal owned by the New Phytologist Trust, a **not-for-profit organization** dedicated to the promotion of plant science, facilitating projects from symposia to free access for our Tansley reviews.
- Regular papers, Letters, Research reviews, Rapid reports and both Modelling/Theory and Methods papers are encouraged. We are committed to rapid processing, from online submission through to publication 'as ready' via *Early View* – our average time to decision is <25 days. There are **no page or colour charges** and a PDF version will be provided for each article.
- The journal is available online at Wiley Online Library. Visit **www.newphytologist.com** to search the articles and register for table of contents email alerts.
- If you have any questions, do get in touch with Central Office (np-centraloffice@lancaster.ac.uk) or, if it is more convenient, our USA Office (np-usaoffice@ornl.gov)
- For submission instructions, subscription and all the latest information visit **www.newphytologist.com**

© 2013 The Authors
New Phytologist © 2013 New Phytologist Trust